A generalized methodology for detection of vascular input function with dynamic contrast enhanced perfusion data

Dattesh D Shanbhag[1], Sandeep N Gupta[2], Kumar T Rajamani[1], Yingxuan Zhu[3], and Rakesh Mullick[4]

[1]*Medical Image Analysis Laboratory, GE Global Research, Bangalore, Karnataka, India,* [2]*Biomedical Image Processing Laboratory, GE Global Research, Niskayuna, NY, United States,* [3]*Image Analytics Laboratory, GE Global Research, Niskayuna, NY, United States,* [4]*GE Global Research, Biosignatures & Signal Processing, Bangalore, Karnataka, India*

Introduction: Dynamic contrast enhancement (DCE) imaging is widely used for studying micro-vascular changes in tumors. The pharmaco-kinetic (pK) model parameters of DCE data are dependent on the choice of vascular input function (VIF) [1]. A manual VIF prescription is time-consuming and introduces inter-observer bias, so an automated VIF detection is desirable. Previous methods for VIF detection involve user-assisted approaches, detect VIF using statistical methods, or use image based vessel geometry markers [2, 3, 4, 5, 6]. In this work we introduce an automated generalized method for detection of VIF with dynamic contrast scans, which takes in to account the prior knowledge about the anatomy, related imaging artifacts and acquisition constraints to provide a consistent estimate of VIF, well-tuned and adaptable for the anatomy being studied. We demonstrate the utility of this method with DCE data for brain and prostate.

Methods and Materials **Patient database:** Data for our study were acquired from patients at multiple centers with appropriate IRBs approving the studies. The database consists of 10 brain and 10 prostate cases. **Imaging:** The datasets were obtained on a 1.5T GE Signa Genesis and 3.0T GE Signa HDx clinical scanners (GE Healthcare, Waukesha, WI). The protocol was: ***a. Brain*:** Axial slices, 3D EFGRE sequence with 8-channel brain coil, TE = 1.15-1.85 ms, TR = 4.9 -5.4 ms, FA = 10°-20°, slice thickness (TH) = 7mm, matrix size = 256 x 256 -512 x 512, FOV = 240x 240 mm^2, 20 bolus volumes ~7s to 14 s / volume. ***b. Prostate*:** Axial slices, 3D FSPGR sequence with EIS TORSO coil, TE = 1.3 ms, TR = 3.8 ms, FA = 15°, TH = 6 mm, matrix size = 256 x256 , FOV = 260 x 260 mm^2, 0.1 mmol/kg Gd-DTPA was injected i.v at 0.3 cc/sec for 100 seconds, 50-65 bolus volumes (~4.5 s/ volume), in 3-5 mins, **Generalized Methodology:** The automated detection of vascular input function(s) involves three major steps [Fig. 1]: ***A. AIF Search Region Slice Localization:*** For the 4D perfusion data (x, y, z, t) loaded into the system, the first step is to localize the slices within which to search for the potential AIF regions. This is based on **a.** Exclusion of slices corrupted by artifacts (e.g. first and last slices due to 3D z-wrap-around); **b.** Accounting for inflow and saturation effects, so that only central or inferior slices are utilized [7]; **c.** Prior anatomical information by use of intrinsic anatomical landmarks or an external atlas registered to the data and **d.** Determining the "slice-goodness" using metrics such as average SNR, and/ or average perfusion curve per slice ($S_{global,\ z\text{-}loc}$ (t)) characteristics such as BAT, auto-correlation etc. In our study, we used conditions (a), (c) and (d) to determine the slices for VIF search regions. ***B. AIF search mask localization***: **a.** Peak slice detection: Within the slices selected in step A, we determine the regions to search for the potential VIFs. For this we use the concept of subtraction angiography to highlight the regions with maximum contrast uptake. We determine the base image $I_{base} = I_{4D}(x, y, z_{loc}, t = 1)$ and the peak image I_{peak}. The peak image is obtained as maximum-intensity projection (MIP) along the time-axis for the particular localized slice (I_{peak}= max ($I_{4D}(x, y, z_{loc}, t = 1 \text{ to } nt)$). For anatomies with bladder in their FOV, the MIP based approach results in large VIF search region mask. In such cases, peak image time-point (t_{peak}) is determined as t_{peak} = min ($_t$ = {max-slope time or peak-time of $S_{global,\ z\text{-}loc}$}). **b**. Subtraction mask generation: The VIF search region image is obtained by $I_{VIF\text{-}search} = I_{peak} - I_{base}$. The gray-scale $I_{VIF\text{-}search}$ image is converted into binary image using multi-label maximum entropy based thresholding algorithm [8]. The number and selection of binary positive labels depend on the anatomy being investigated. We set number of labels to three for thresholding. In brain we retained only label 3 (highest intensity), while for prostate, we retained label = 2 and 3, for creating a binary mask **c.** Anatomy-specific mask refinement: In prostate, the bright region around the ER coil is detected within the binary mask, which increases the compute time for VIF search and result in potential false-positives. For this we have implemented a phase-field based segmentation, combined with image geometry and context information on the I_{base} image to remove the bright regions around the ER-coil and retain the vascular enhancing regions in prostate (Fig. 2) [9]. ***C.AIF detection using shape based statistics*:** We now proceed to determine the various shape parameters such as BAT, TTP, and Full-width at 80% max, curve-cutoff, upslope, and downslope for each signal time curve in the VIF mask search region (Figure 3). These curves are ranked for each of the shape parameter using a 5-class cluster and cumulative score determined for each curve. The ones with lowest score are chosen to be the potential VIF. The weights for the cumulative score of each parameter were adjusted depending on the anatomy. For e.g. in neuro, with sagittal sinus being the desired VIF, we provide less weight to FW80Max and TTP so that veins are not weighted less compared to arteries. To avoid spurious false-positives, the potential VIFs are cross-correlated to allow only those with maximum cross-correlation coefficients (> 95%) to be reported as detected VIFs. We restrict the number of VIF to top 5 or less correlating curves. While we have used a signal shape parameters based ranking approach within this module, this can be substituted with other approaches as reported earlier [6, 7]. The cumulative average of the detected VIFs was converted to concentration as described in [1]. The entire workflow was implemented using the functionality available in the Insight Toolkit (ITK) [10].**Validation:** A trained radiologist, blinded to our study results, marked a single VIF location after evaluating multiple signal curves within the 4D DCE data for each case. For brain cases, the VIF location was marked in sagittal sinus vein, and for the prostate cases in the femoral artery. For each of the manual and automated AIF signal curve, we calculated the BAT and TTP indices. Each of the manually marked VIF was converted into concentration curve. Evaluation metric consisted of correlation coefficient between manual and automated AIF signal curves and calculation of intra-class correlation coefficient (ICC) for BAT, TTP and peak concentration values. Statistical analysis was performed with MedCalc®(v. 10.4) software.

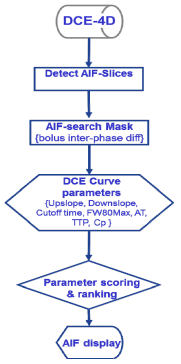

Figure 1. Generalized VIF detection workflow

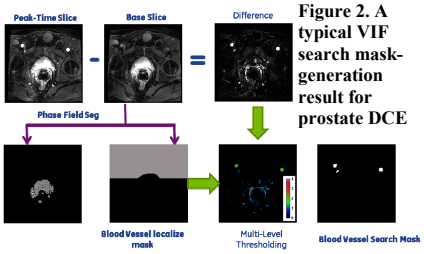

Figure 2. A typical VIF search mask-generation result for prostate DCE

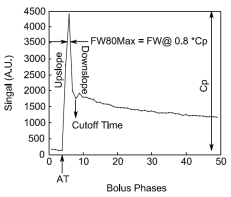

Figure 3. The shape parameters which describe the VIF curve

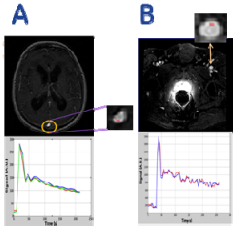

Figure 4, Typical VIF located with automated workflow

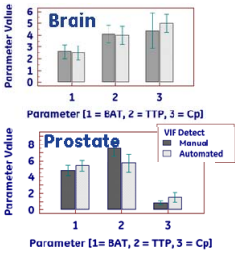

Figure 5. BAT, TTP and Cp for manual and auto VIF methods

Results and Discussion: For both neuro and prostate cases, the automated algorithm consistently picked up VIF in sagittal sinus and femoral artery region (Figure 4). Therefore we observed excellent correlation (0.97) between the VIF marked manually and determined using the automated algorithm. Among the parameters describing the VIF, BAT and TTP matched best between manual and automated approach (ICC > 0.95), while differences were observed for the peak values (ICC ~ 0.65) (Fig. 5). The differences in peak values were primarily due to the fact that saturation and to some extent TOF effects affect the signal to concentration conversion and result in very high (> 15-20 mM) concentration values. Therefore in case of manual VIF search, a better workflow would be to mark the VIF on concentration curves, compared to signal curves. While we have demonstrated the technique for DCE data with prostate and brain cases, the approach can be easily extended to breast, ovarian and uterine data as well. Moreover the technique can also be applied for VIF detection with other dynamic perfusion data approaches such as DSC imaging as well.

Conclusions: We have introduced a completely automated workflow for detection of VIFs for DCE perfusion data, which provides a reliable and consistent location of VIF, well suited to anatomy being studied.

Acknowledgments: We will like to thank Dr. Fiona Fennessy (Brigham and Women's Hospital, Boston) and Dr. Adilson Prando (Ressonancia Magnetica Campinas, Brazil) for providing the data used for these experiments.**References:** **[1].** Tofts et.al. JMRI 1999;10(3):223-232. **[2].** Parker et.al. Proc. ISMRM 2003, p1264 **[3].** Chen et.al. MICCAI, 11: 594-601 **[4].** Li et.al. Phys. Med. Biol. 56 (2011) 5753–5769, **[5].** Rijpkema M et.al., JMRI(2001) 14:457–463 **[6].** Murase et.al. JMRI 13:797–806 (2001), **[7].** Cron et.al., MRM 66(2):498-504 **[8].** LuessiM et.al., Electronic Imaging, v 18, no. 1, (Jan-Mar 2009)(p. 013004-1 - 013004-10). **[9].** Samson et al. PAMI, v. 22(5), May 2000 **[10].** http://www.itk.org.